



Competitive Biosorption of Rare-earth Elements on Bacterial Biomass: Equilibrium and Kinetic Studies

C.S. Jordão ¹, E.C. Giese ^{1, *}

¹ Center for Mineral Technology (CETEM), Av. Pedro Calmon 900, CEP 21941 908, Rio de Janeiro, Brazil.

* Corresponding author email: egiese@cetem.gov.br

DOI: <https://doi.org/10.54392/irjmt2244>

Received: 28-03-2022; Revised: 21-07-2022; Accepted: 23-07-2022; Published: 29-07-2022



Abstract: Previous studies showed that chemical modified *Bacillus subtilis* biomass possessed the high potential for recovery rare-earth elements, and, in this study, mathematical models were applied to explain the *B. subtilis* biomass La³⁺ and Sm³⁺ ions sorption capacity. The experimental isotherm data were analyzed using Langmuir, Freundlich, Temkin, and DRK equations. Both Langmuir and Freundlich isotherms models that fit the equilibrium data. Temkin model showed that it occurs physisorption. In more dilute solutions, the adsorption preference follows the order La³⁺ > Sm³⁺. With the increase in the concentration of rare-earth elements, there is an inversion in the preference for Sm³⁺ > La³⁺. The results demonstrate that the optimum model for describing the kinetics of the biosorption of both rare-earth elements is the pseudo-second-order model as well as the viability of recovering lanthanum using bacterial biomass sorbents, a practical technique.

Keywords: Adsorption Equilibrium, Adsorption Kinetics, Bacillus Subtilis, Rare Earth Elements

1. Introduction

A gram-positive bacterium called *Bacillus subtilis* has a cell wall made up largely of peptidoglycan and teichoic acid. These functional carbohydrates have functional groups with pKa values of 4.8, 6.9, and 9.4 that confer three unique organic functional surfaces. These functional groups include carboxylic, phosphoric, and hydroxyl functional groups [1, 2]. *B. subtilis* has a unique binding site for rare-earth elements, which has a stronger affinity for heavy rare-earth elements (Tm, Yb, and Lu) and a lesser affinity for light rare-earth elements (La, Nd, and Pd), especially when the biosorption process is carried out in the pH range between 2.5 and 5 [3]. Because rare-earth elements bind to the active sites of *B. subtilis* through the formation of complexes with phosphate groups by phosphoester-type interactions, which have a higher number of coordination, this preference in biosorption happens [4].

The lanthanide family (Z = 57 to 71) contains 17 elements that make up the rare-earth elements, including yttrium (Z = 39) and scandium (Z = 21), which have remarkably comparable chemical and physical characteristics. Because of the nature of its electronic configurations, which provide a very stable 3+ oxidation state, there is a high degree of similarity [5, 6]. The gram-negative bacteria *Leisingera methylohalidivorans* and *Phaeobacter inhibes* and other microorganisms have been described as having lower selectivity to ytterbium (Yb) and lutetium (Lu) than *B. subtilis* [7]. In contrast, chemically modified free *B. subtilis* cells displayed

extremely high levels of light rare-earth elements removal, reaching up to 99% in diluted solutions [9].

By passively attaching to active, or dead, biomass materials in aqueous solutions, rare-earth elements are removed through the sorption process known as biosorption. Adsorption, absorption, reduction, methylation, and oxidation are some of the mechanisms involved in biosorption. The rare earth elements can bind to oxygen donor atom groups that are present in the microbial species' cell-wall, making biosorption comparable to an ion-exchange mechanism [10, 11]. The considerable economic value and numerous industrial uses make biorecovery of rare-earth elements through biosorption appealing. Thus, the biosorption serves as an outstanding cost-effective method for the recovery of rare earth metals from aqueous solutions and a biotechnological innovation [12-14].

Lanthanum (La, Z = 57) is the lightest rare earth. This TR is used in the manufacture of special optical glasses, such as infrared absorber glass. Due to its high refractive index and low dispersion rates, lanthanum is used as a doping agent in camera and telescope lenses. It is also used in matches for fluorescent lamps and LED lamps [15]. Samarium (Sm, Z = 62) is used for doping calcium chloride crystals for use in optical lasers. It is also used in infrared absorbent glass and as a neutron absorber in nuclear reactors [16]. Therefore, this investigation's main objective was to evaluate several

mathematical models on the equilibrium and kinetics of biosorption of La^{3+} and Sm^{3+} ions from diluted solutions by the suspension of *B. subtilis* cells to realize the adsorption mechanisms involved in this bioprocess.

2. Material and Methods

2.1 Materials

La^{3+} and Sm^{3+} stock solutions (5 g L^{-1}) were prepared by dissolving rare-earth element oxides (Pacific Industrial Development Corporation, Weihai, China) in a solution of deionized water and nitric acid. These stock solutions were then diluted to the concentrations needed for the experiments listed below.

2.2 Microorganism and media

The microorganism was grown in accordance with Giese and Jordão [9]. The *B. subtilis* cells were pre-treated with 50 mL sodium hydroxide solution (1.0 M) for 30 min at room temperature in 125-mL Erlenmeyer flasks in a rotary shaker at 100 rpm at 30 °C after being washed with deionized water. The pre-treated sedimented cells that were recovered after centrifugation (1,500 g/15 min) were employed as the biosorbent material.

2.3 Biosorption experiments

The pre-treated *B. subtilis* cells (1.0 g (dry wt. cell) L^{-1}) were added to 50 mL of ionic solutions of La^{3+} or Sm^{3+} (15 mg L^{-1}) at pH 3.0 in 125 mL Erlenmeyer flasks to conduct the kinetic investigations. The flasks were kept at 5, 10, 20, 30, 40, 50, and 60 minute contact times. The starting concentrations of La^{3+} and Sm^{3+} at 10, 25, 40, 50, and 75 mg L^{-1} at a 20-minute contact duration were individually assessed for equilibrium experiments. The average findings of the two biosorption studies, which were performed, are shown. The samples were centrifuged for 15 minutes at 1,500 g, and the clear supernatant's lanthanide ion concentration was determined. By using inductively-coupled plasma atomic emission spectrometry, the La^{3+} and Sm^{3+} were identified (ICP-OES Perkin Elmer, OPTIMA3000, USA).

2.4 Langmuir isotherm

Equation 1 expresses the linearized Equation and the monolayer coverage of La^{3+} onto *B. subtilis* cells that is predicted by the Langmuir [17] isotherm.

$$\frac{1}{q_e} = \frac{1}{Q_m} + \frac{1}{Q_m K_L C_e} \quad (1)$$

where Q_m is the maximum monolayer coating capacity (mg g^{-1}), C_e is the equilibrium adsorbate concentration (mg L^{-1}), q_e is the quantity adsorbed per gram of adsorbent (mg g^{-1}), and K_L is the Langmuir constant of the theoretical adsorption capacity in the monolayer (L mg^{-1}).

2.5 Freundlich isotherm

The reversible biosorption is explained by Freundlich's [18] isotherm, which postulates a multilayer attraction of La^{3+} onto *B. subtilis* cells. The linearized Equation 2 can be used to describe the nonlinear form of the Freundlich isotherm. (2)

$$\ln q_e = \ln K_F + \frac{1}{n} \ln C_e \quad (2)$$

where n is a parameter that refers to the strength of La^{3+} binding to *B. subtilis* cells and K_F (mg^(1-1/n)L^{1/n} g⁻¹) is the Freundlich model constant.

2.6 Dubinin-Radushkevich model

Equation 3 describes of the Gaussian energy distribution onto the biosorbent in the Dubinin-Radushkevich (DRK) model [19] is used to explain the La^{3+} biosorption system:

$$q_e = q_s \exp \left[-\beta \left(RT \ln \left(1 + \frac{1}{C_e} \right) \right)^2 \right] \quad (3)$$

where q_s is the theoretical monolayer saturation capacity represented by the DRK constant, and is the adsorption energy constant (kJ² mol⁻¹).

2.7 Temkin model

Temkin model [20] presupposes that the heat of biosorption reduces as La^{3+} biosorption uptake decreases, and Equation 4 defines the linear form:

$$q_e = \left(\frac{RT}{H} \right) \ln K_T + \left(\frac{RT}{H} \right) \ln C_e \quad (4)$$

where K_T is the Temkin constant (L g^{-1}).

2.8 Pseudo-first order model

Kinetic analysis of pseudo-first-order was performed using Equation 5 [21]:

$$\ln(q_e - q_t) = \ln q_e - k_1 t \quad (5)$$

where the constant k_1 is the first order of adsorption (g $\text{mg}^{-1} \text{min}^{-1}$), and q_e and q_t are the amounts adsorbed (mg g^{-1}) at equilibrium and at time t (min), respectively.

2.9 Pseudo-second order model

Kinetic analysis of pseudo-second-order was performed using Equation 6 [22]:

$$\frac{t}{q_t} = \frac{1}{k_2 q_e^2} + \frac{t}{q_e} \quad (6)$$

where the constant k_2 is the second order of adsorption (g $\text{mg}^{-1} \text{min}^{-1}$), and q_e and q_t are the amounts adsorbed (mg g^{-1}) at equilibrium and at time t (min), respectively.

2.10. Elovich model

The Elovich kinetic model can be represented by Equation 7 [21]:

$$q_t = \frac{1}{b} \ln(ab) + \frac{1}{b} \ln(t) \quad (7)$$

where b is the constant of desorption (mg g^{-1}), a is the initial rate of adsorption ($\text{g mg}^{-1} \text{min}^{-1}$), and q_t is the amount adsorbed (mg g^{-1}) at time t (min).

2.11 Weber and Morris intraparticle diffusion model

According to Weber and Morris [23], if intraparticle diffusion is the determinant of speed, removing the adsorbate varies with the square root of time. Thus, the intraparticle diffusion model can be expressed by Equation 8:

$$q_t = k_{dif} t^{\frac{1}{2}} + C \quad (8)$$

where the intra-particle diffusion rate constant ($\text{mg g}^{-1} \text{min}^{-1/2}$), which may be calculated from the slope of the linear plot of q_t vs $t^{1/2}$, and C is the intercept. The boundary layer thickness is determined by the C value values; the larger the intercept, the more significant the boundary layer effect [24].

2.12 Boyd model

Boyd's Equation predicts the limiting step involved in the adsorption process for different systems, is described by Equation 9 [25]:

$$B_t = -0,4977 - \ln\left(1 - \frac{q_t}{q_e}\right) \quad (9)$$

where q_e is the amount of metal ions adsorbed at an infinite time (mg g^{-1}), q_t is the amount of metal ions adsorbed at time t , and B_t is a mathematical function used to plot the graph B_t versus t .

3. Results and discussion

The biosorption of La^{3+} and Sm^{3+} by *B. subtilis* cells in relation to metal concentration was investigated. The amount of La^{3+} and Sm^{3+} adsorbed on *B. subtilis* cells (mg g^{-1}) increased with the initial concentrations of these rare-earth ions, as seen in Fig. 1. The impact of La^{3+} and Sm^{3+} starting concentrations on *Botryosphaeria rhodina* biomass has previously been examined by Giese *et al.* [26]. As the initial concentration of the adsorbate increased, the biosorption effectiveness of rare-earth ions to the fungal biomass dropped. The increase in ions vying for the available binding sites, which results in the saturation of active sites, can be used to explain this tendency. Similar outcomes were observed for the adsorption of La^{3+} and Sm^{3+} on the biomass of the fungus *Penicillium simplicissimum* and La^{3+} and Ce^{3+} on the powdered leaf of *Platanus orientalis* [27, 28].

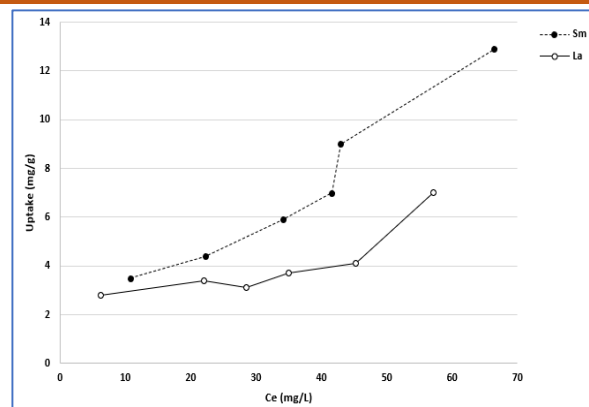


Figure 1 Effect of initial concentration on the biosorption of La^{3+} and Sm^{3+} by *Bacillus subtilis* cells.

Table 1 lists the correlation coefficient (R^2) and the constants for the Langmuir, Freundlich, Temkin, and DRK models. The sorption characteristics of La^{3+} and Sm^{3+} on *B. subtilis* biomass appear to follow both adsorption models, according to a comparison of the Langmuir and Freundlich isotherm models (Figs. 2 and 3). La^{3+} and Sm^{3+} cells of *B. subtilis* have maximal absorption capacities (Q_0) of 9.49 mg g^{-1} and 32.57 mg g^{-1} , respectively. According to preference tests carried out by Martinez *et al.* [3], certain locations in the cell wall of *B. subtilis* have a lower affinity for light rare-earth elements, which is in line with the preference shown by Sm^{3+} ions.

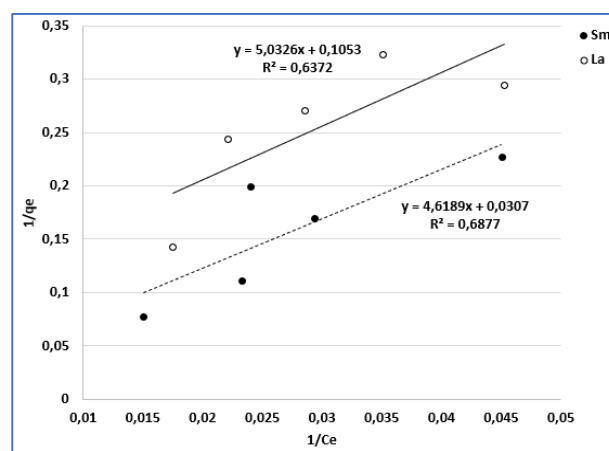


Figure 2 Langmuir sorption isotherm of La^{3+} and Sm^{3+} by *Bacillus subtilis* cells.

La^{3+} ions have an R_L value of 0.43 while Sm^{3+} ions have an R_L value of 0.65. These numbers demonstrate that under the experimental circumstances investigated, the biosorption of La^{3+} and Sm^{3+} onto *B. subtilis* cells is advantageous ($0 > R_L > 1$). Small K_L values suggested a minimal interaction between *B. subtilis* cells and rare-earth ions.

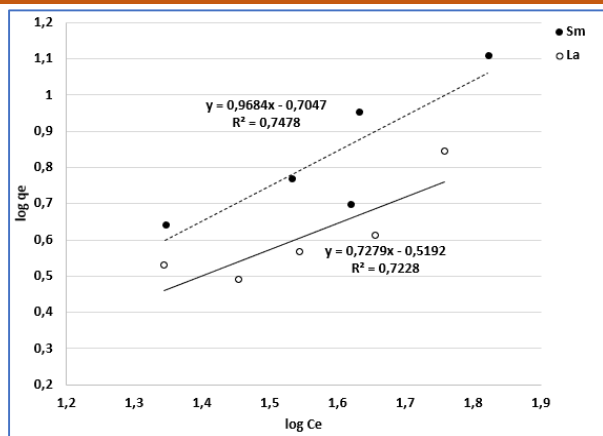


Figure 3 Freundlich sorption isotherm of La^{3+} and Sm^{3+} by *Bacillus subtilis* cells.

Table 1 Isotherm model constants and correlation coefficients for La^{3+} and Sm^{3+} biosorption by *Bacillus subtilis* cells (pH 3, 60 min, 1 mg mL⁻¹ and 30 °C).

| | La^{3+} | Sm^{3+} |
|------------------------------------|------------------|------------------|
| Langmuir model | | |
| Q_o (mg/g) | 9.49 | 32.57 |
| K_L (L/mg) | 0.02 | 0.01 |
| R_L | 0.43 | 0.65 |
| R^2 | 0.637 | 0.688 |
| Freundlich model | | |
| K_F (mg/g)/(mg/L) ^{1/n} | 0.30 | 0.19 |
| 1/n | 0.73 | 0.97 |
| n | 1.37 | 1.03 |
| R^2 | 0.723 | 0.745 |
| Temkin model | | |
| B | 21.50 | 28.96 |
| A_T (L/g) | 0.17 | 0.11 |
| B_T (J/mol) | 115.22 | 85.56 |
| R^2 | 0.889 | 0.917 |
| DRK model | | |
| Q_s | 0.61 | 0.41 |
| Kad | 9.00E-09 | 2.00E-08 |
| E | 1.05E+04 | 7.07E+03 |
| R^2 | 0.658 | 0.658 |

According to the Freundlich model, the value of n determines whether the process is more apt to chemisorb ($n < 1$) or physisorb ($n > 1$). According to this study, rare-earth ions biosorbed onto *B. subtilis* cells with $n = 1.37$ for La^{3+} and $n = 1.03$ for Sm^{3+} . Weak electrostatic interactions such as London forces, dipole-dipole forces, and the Van der Waals link between the adsorbent and adsorbate are what cause the physisorption to occur. The measured results, however, showed a weak adsorption intensity [29]. In Table 1 the results for Temkin isotherm are also given (Fig. 4).

The rare-earth ions biosorption onto *B. subtilis* cells is an exothermic reaction since B_T is positive. Given that the values of B_T are both less than 8 kJ/mol, the interactions between bacterial cells and La^{3+} and Sm^{3+} are weak, as indicated before by Langmuir and Freundlich isotherms. It is possible to conclude that both

rare-earth ions biosorption mechanism is a reversible ion exchange with active sites present in bacterial cells.

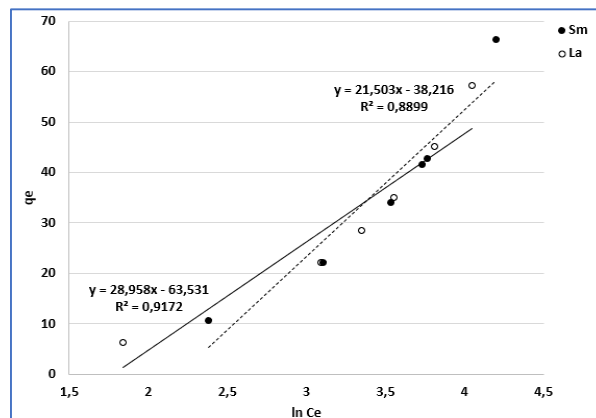


Figure 4 Temkin sorption isotherm of La^{3+} and Sm^{3+} by *Bacillus subtilis* cells.

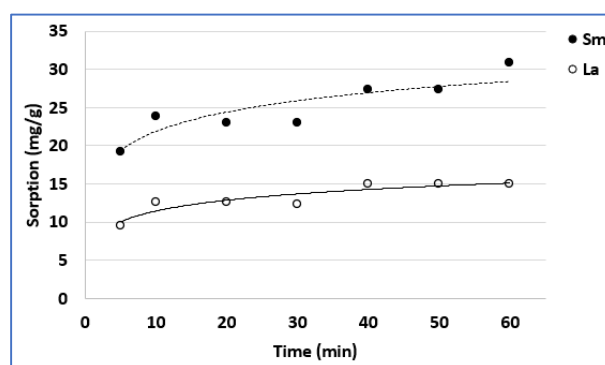


Figure 5 Adsorption kinetics of La^{3+} and Sm^{3+} by *Bacillus subtilis* cells at different concentrations.

The kinetic study supports the study of equilibrium under specific experimental conditions. The kinetics parameters are essential for using adsorbents so that the process happens as quickly as possible and efficiently as possible, saving time and costs [30]. Several models have been used to determine the limiting step in the mechanism or process. The following kinetic and diffusion models were studied in this work: Pseudo-first order; Pseudo-second order, Elovich equation, and intraparticle diffusion models [21-23, 25].

Figure 5 depicts the kinetics of La^{3+} and Sm^{3+} adsorption on *B. subtilis* biomass. For both the La^{3+} and Sm^{3+} ions systems, it was found that the adsorption equilibrium period was quick, occurring within the first 40 min. The similar result was seen in a study where activated charcoal was used to adsorb La^{3+} ions. After 30 minutes, the amount of La^{3+} adsorbed increased to more than 135 mg g⁻¹, and after 60 minutes, the maximum level of adsorption was obtained at 144.80 mg g⁻¹ [31]. According to this study, *B. subtilis* was able to absorb both rare earth elements to their maximum capacity, 30 mg g⁻¹ for Sm^{3+} and 15 mg g⁻¹ for La^{3+} within 60 minutes.

Besides being beneficial to the process of biosorption, the short time needed for achieving

conditions of equilibrium is regarded as an indicator of the *B. subtilis* cells/ La^{3+} , and Sm^{3+} ions adsorption systems are more dominated by chemical interactions than by diffusion [32]. Sousa *et al.* [33] used green coconut shell powder that has been processed for the adsorption of hazardous metals from wastewater and reported similar results. This implies that physical-chemical interactions between the adsorbent and the adsorbate in solution are what cause the adsorption.

Table 2 Kinetic constants and correlation coefficients for La^{3+} and Sm^{3+} biosorption by *Bacillus subtilis* cells (pH 3, 60 min, 1 mg mL^{-1} , and 30 °C).

| | La^{3+} | Sm^{3+} |
|--------------------------------|------------------|------------------|
| Pseudo-first order | | |
| q_e (mg/g) | 0.98 | 0.96 |
| k_1 (min^{-1}) | 1.44 | 2.38 |
| R^2 | 0.750 | 0.783 |
| Pseudo-second order | | |
| q_e (mg/g) | 0.31 | 0.24 |
| k_2 (min^{-1}) | 0.06 | 0.03 |
| R^2 | 0.946 | 0.953 |
| Elovich model | | |
| a (mg/g.min) | 54.33 | 3.66 |
| b (g/mg) | 0.49 | 0.11 |
| R^2 | 0.825 | 0.786 |
| Intraparticle diffusion | | |
| k_{dif} | 0.89 | 0.18 |
| C | 6.49 | 1.61 |
| R^2 | 0.799 | 0.668 |

second-order model. ($R^2 = 0.946$ to La^{3+} and $R^2 = 0.953$ to Sm^{3+}), compared to the first-second order ($R^2 = 0.750$ to La^{3+} and $R^2 = 0.783$ to Sm^{3+}) and Elovich model ($R^2 = 0.825$ to La^{3+} and $R^2 = 0.786$ to Sm^{3+}). Fig. 6 shows the models corresponding to the pseudo-second-order and the Elovich equation of the *B. subtilis*/ La^{3+} and Sm^{3+} mono-elementary systems. The rate-limiting step may involve chemical sorption or chemisorption, which uses valency forces to share or exchange electrons between rare-earth elements and bacterial cells. This is suggested by the better fit of the pseudo-second-order model. The same observation about freshwater algae's La^{3+} recovery was discovered [34].

The plot of (t/q_t) against (t) yielded the value of the sorption rate constant (k_2) for La^{3+} and Sm^{3+} biosorption by *B. subtilis* (Fig. 6A). It should be observed that the rate constant (k_2) of La^{3+} was more significant than that of Sm^{3+} , indicating that the adsorption rate of La^{3+} ions was marginally higher at the concentration under study (15 mg L^{-1}). These findings were supported by the parameter a in the Elovich equation, which showed that the initial adsorption rate for La^{3+} was higher than that for Sm^{3+} (54.3 mg $\text{g}^{-1} \text{min}^{-1}$) (3.6 mg $\text{g}^{-1} \text{min}^{-1}$). This suggests that as contact duration increases, the La^{3+} ions' affinity for the surface of *B. subtilis* cells increases. This fact was proven by utilizing *Turbinaria conoides*, a brown sea alga, where the uptake levels followed the hierarchy of $\text{La}^{3+} > \text{Ce}^{3+} > \text{Eu}^{3+} > \text{Yb}^{3+}$ [35]. The plot of (q) against $\ln(t)$ yielded the values of the Elovich parameters a and b (Fig. 6B).

In order to understand the processes and rate-controlling strategies impacting the adsorption kinetics, the experimental kinetic results were fitted to the Weber intraparticle diffusion [23] and Boyd model [25]. According to Eq. (4), the La^{3+} and Sm^{3+} biosorption data were plotted (data not shown). Over the whole time period, the points were not linear ($R^2 = 0.799$ to La^{3+} and $R^2 = 0.668$ to Sm^{3+}), indicating that the adsorption process was influenced by many mechanisms. This anomaly might be explained by the difference in mass transfer rates between the first and last stages of rare-earth element biosorption, indicating that there were other rate-limiting factors at play in this bioprocess besides diffusion into pores.

4. Conclusion

The current study provided additional proof that using *Bacillus subtilis* biomass as an adsorbent, it was possible to use an adsorption technique to remove the rare earth elements La^{3+} and Sm^{3+} ions from aqueous solutions. Both the Langmuir and Freundlich isotherm models can describe how La^{3+} and Sm^{3+} ions adsorb to bacterium biomass, showing that adsorption primarily takes place on the multilayers and heterogeneous surfaces of the cell wall. The kinetics of La^{3+} and Sm^{3+} on *B. subtilis* biomass were attributed to many mechanisms, and the process is non-rate limiting. The

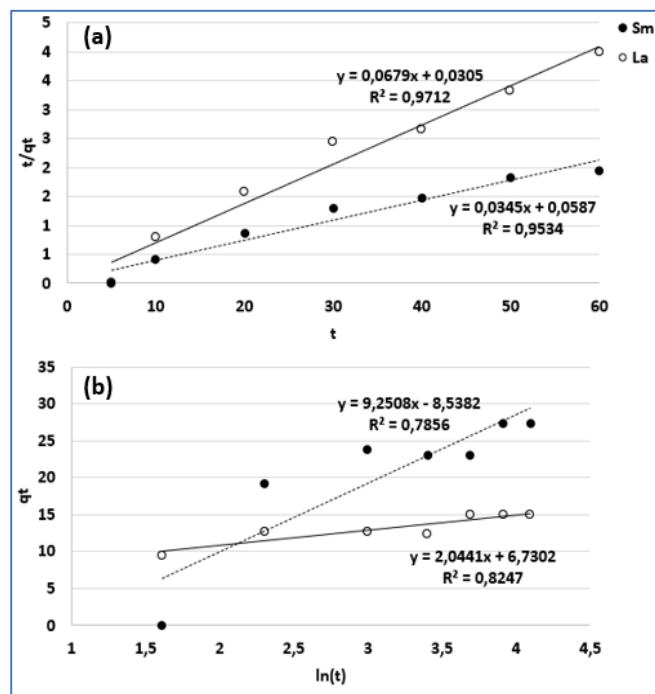


Figure 6 Kinetic models of biosorption of La^{3+} and Sm^{3+} by *Bacillus subtilis* cells. (A) Pseudo-second order plot and (B) Elovich equation plot.

The kinetic parameters for each model using the linear technique are shown in Table 2. The experimental value was more accurately approximated by the pseudo-

biosorption is controlled by pseudo-second-order kinetics.

References

- [1] J.B. Fein, C.J. Daughney, N. Yee & T. Davis, A chemical equilibrium model for metal adsorption onto bacterial surfaces. *Geochimica et Cosmochimica Acta*, 61(1997) 3319-3328. [\[DOI\]](#)
- [2] Y.G. Liu, T. Liao, Z.B. He, T.T. Li, H. Wang, X.J. Hu, Y.M. Guo & Y. He. Biosorption of copper(II) from aqueous solution by *Bacillus subtilis* cells immobilized into chitosan beads. *The Transactions of Nonferrous Metals Society of China*, 23 (2013) 1804-1814. [\[DOI\]](#)
- [3] R.E. Martínez, O. Pourret & Y. Takahashi, Modeling of rare earth element sorption to the Gram-positive *Bacillus subtilis* bacteria surface. *The Journal of Colloid and Interface Science*, 413 (2014) 106-111. [\[DOI\]](#)
- [4] Y. Takahashi, T.X. Chatellier, K.H. Hattori, K. Kato & D. Fortin, Adsorption of rare earth elements onto bacterial cell walls and its implication for REE sorption onto natural microbial mats. *Chemical Geology*, 219 (2005) 53-67. [\[DOI\]](#)
- [5] A.R. Richard & M. Fan, Rare earth elements: Properties and applications to methanol synthesis catalysis via hydrogenation of carbon oxides. *Journal of Rare Earths*, 36 (2018) 1127-1135. [\[DOI\]](#)
- [6] C.L. Owens, G.R. Nash, K. Hadler, R.S. Fitzpatrick & F. Wall, Apatite enrichment by rare earth elements: A review of the effects of surface properties. *Advances in Colloid and Interface Science*, 265 (2019) 14-28. [\[DOI\]](#)
- [7] A. Breuker, S.F. Ritter & A. Schippers, Biosorption of rare earth elements by different microorganisms in acidic solutions. *Metals*, 10 (2020) 954. [\[DOI\]](#)
- [8] N.V. Coimbra, F.S. Gonçalves, M. Nascimento & E.C. Giese, Study of adsorption isotherm models on rare earth elements biosorption for separation purposes, *International Journal of Materials and Metallurgical Engineering*, 13 (2019) 86.
- [9] E.C. Giese & C.S. Jordão, Biosorption of lanthanum and samarium by chemically modified *Bacillus subtilis* free cells. *Applied Water and Science*, 9 (2019) 182. [\[DOI\]](#)
- [10] N.K. Gupta, A. Sengupta, A. Gupta, J.R. Sonawane & H. Sahoo, Biosorption - an alternative method for nuclear waste management: A critical review. *Journal of Environmental Chemical Engineering*, 6 (2018) 2159-2175. [\[DOI\]](#)
- [11] E.C. Giese, D.D.V. Silva, A.F.M. Costa, S.G.C. Almeida & K.J. Dussán, Immobilized microbial nanoparticles for biosorption. *Critical Reviews in Biotechnology*, 40 (2020) 653-666. [\[DOI\]](#)
- [12] N. Das & D. Das, Recovery of rare earth metals through biosorption: An overview. *Journal of Rare Earths*, 31 (2013) 933-943. [\[DOI\]](#)
- [13] E.C. Giese, Biosorption as green technology for the recovery and separation of rare earth elements. *World Journal of Microbiology and Biotechnology*, 36 (2020) 52. [\[DOI\]](#)
- [14] E.C. Giese, Mining applications of immobilized cells in alginate matrix: an overview. *Revista Internacional de Contaminación Ambiental*, 36 (2020) 775-787. [\[DOI\]](#)
- [15] R.P. Weeden, B. Berlinger & J. Aaseth, Lanthanum. *Handbook of the Toxicology of Metals*, 2 (2015) 903-909.
- [16] Y. Ma, X. Wang, S. Li, M.S. Toprak, B. Zhu & M. Muhammed, Samarium-doped ceria nanowires: novel synthesis and application in low-temperature solid oxide fuel cells. *Advanced Materials*, 22 (2010) 1640-1644. [\[DOI\]](#)
- [17] I. Langmuir, Adsorption of gases on plane surfaces of glass, mica and platinum. *Journal of the American Chemical Society*, 40 (1918) 1361-1403. [\[DOI\]](#)
- [18] H. Freundlich, Over the adsorption in solution. *The Journal of Physical Chemistry*, 57 (1906) 384-410. [\[DOI\]](#)
- [19] A. Dabrowski, Adsorption-from theory to practice. *Advances in Colloid and Interface Science*, 93 (2001) 135-224. [\[DOI\]](#)
- [20] K.A.M. Said, N.Z. Ismail, R.L. Jama'in, N.A.M. Alipah, N.M. Sutan, G.G. Gadung, R. Bains & N.S.A. Zauz, Application of Freundlich and Temkin isotherm to study the removal of Pb(II) via adsorption on activated carbon equipped polysulfone membrane. *International Journal of Engineering and Technology*, 7 (2018) 91-93. [\[DOI\]](#)
- [21] L. Largitte & R. Pasquier, A review of the kinetics adsorption models and their application to the adsorption of lead by an activated carbon. *Chemical Engineering Research and Design*, 109 (2016) 495-504. [\[DOI\]](#)
- [22] Y.S. Ho & G. Makay, Sorption of dye from aqueous solution by peat. *Chemical Engineering Journal*, 70 (1998) 115-124. [\[DOI\]](#)
- [23] W.J. Weber Jr. & J.C. Morris, Kinetics of adsorption on carbon from solution, *Journal of the Sanitary Engineering Division*, 89 (1963) 31-39.
- [24] D. Kavitha & C. Namasivayam, Experimental and kinetic studies on methylene blue adsorption by coir pith carbon. *Bioresource Technology*, 98 (2007) 14-21. [\[DOI\]](#)
- [25] G.E. Boyd, J. Schubert & A.W. Adamson, The exchange adsorption of ions from aqueous solutions by organic zeolites, I: Ion exchange equilibrium. *Journal of the American Chemical Society*, 69 (1947) 2818-2829. [\[DOI\]](#)

- [26] E.C. Giese, A.M. Barbosa-Dekker & R.F.H. Dekker, Biosorption of lanthanum and samarium by viable and autoclaved mycelium of *Botryosphaeria rhodina* MAMB-05. *Biotechnology Progress*, (2019) e2783. [\[DOI\]](#)
- [27] Ş. Sert, C. Kütahyalı, S. İnan, Z. Talip, B. Çetinkaya & M. Eral, Biosorption of lanthanum and cerium from aqueous solutions by *Platanus orientalis* leaf powder. *Hydrometallurgy*, 90 (2008) 13-18. [\[DOI\]](#)
- [28] L.R. Bergsten-Torralba, C.R.S. Nascimento, D.F. Buss & E.C. Giese, Kinetics and equilibrium study for the biosorption of lanthanum by *Penicillium simplicissimum* INCQS 40,211.3 *Biotech*, 11 (2021) 460. [\[DOI\]](#)
- [29] M.A. Al-Ghouti & D.A. Da'ana, Guidelines for the use and interpretation of adsorption isotherm models: A review. *Journal of Hazardous Materials*, 393 (2020) 122383. [\[DOI\]](#)
- [30] R.N.P. Teixeira, V.O. Sousa Neto, J.T. Oliveira, T.C. Oliveira, D.Q. Melo, M.A.A. Silva & R.F. Nascimento, Study on the use of roasted barley powder for adsorption of Cu²⁺ ions in batch experiments and in fixed-bed columns. *BioResources*, 8 (2013) 3556-3573. [\[DOI\]](#)
- [31] H.M. Marwani, H.M. Albishri, T.A. Jalal & E.M. Soliman, Study of isotherm and kinetic models of lanthanum adsorption on activated carbon loaded with recently synthesized Schiff's base. *Arabian Journal of Chemistry*, 10 (2017) S1032-S1040. [\[DOI\]](#)
- [32] M.X. Loukidou, T.D. Karapantsios, A.I. Zouboulis & K.A. Matis, Diffusion kinetic study of cadmium(II) biosorption by *Aeromonas caviae*. *Journal of Chemical Technology & Biotechnology*, 7 (2004) 711-719. [\[DOI\]](#)
- [33] F.W. Sousa, A.G. Oliveira, J.P. Ribeiro, M.F. Rosa, D. Keukeleire & R.F. Nascimento, Green coconut shells applied as adsorbent for removal of toxic metal ions using fixed-bed column technology. *Journal of Environmental Management*, 91 (2010) 1634-1640. [\[DOI\]](#)
- [34] Z.S. Birungi & E.M.N. Chirwa, The kinetics of uptake and recovery of lanthanum using freshwater algae as biosorbents: Comparative analysis. *Bioresource Technology*, 160 (2014) 43-51. [\[DOI\]](#)
- [35] K. Vijayaraghavan, M. Sathishkumar & R. Balasubramanian, Biosorption of lanthanum, cerium, europium, and ytterbium by a brown marine alga, *Turbinaria Conoides*. *Industrial & Engineering Chemistry Research*, 49 (2010) 4405-4411. [\[DOI\]](#)

Acknowledgement

C.S. Jordão is grateful for the scientific initiation scholarship granted by CNPq/PIBIC/CETEM.

Author's contribution

Caio S. Jordão carried out the experiments. **Ellen C. Giese** conceived the original idea, supervised the project and wrote the manuscript.

Conflict of interest

The Authors have no conflicts of interest to declare that they are relevant to the content of this article.

Does this article screened for similarity?

Yes

About the License

© The Author(s) 2022. The text of this article is open access and licensed under a Creative Commons Attribution 4.0 International License.